I. J. Engineering and Manufacturing, **2025, 2, 36-45**
Published Online on April 8, 2025 by MECS Press (http://www.mecs-press.org/)
DOI: 10.5815/ijem.2025.02.03

Optimized Ambipolar Characteristics in Charge Plasma-Doped InGaAs/GaAs TFET Biosensors with Dual Metal Gate

Soumya Sen
Department of Computer Science & Engineering, University of Engineering & Management, Jaipur, Rajasthan-303807, India
E-mail: soumya.sen@uem.edu.in
ORCID iD: https://orcid.org/0000-0002-6354-5206

Angshuman Khan*
Department of Electronics & Communication Engineering, University of Engineering & Management, Jaipur, Rajasthan-303807, India
E-mail: angshuman.khan@uem.edu.in
ORCID iD: https://orcid.org/0000-0002-1298-628X
*Corresponding Author

Received: 13 May, 2024; Revised: 08 June, 2024; Accepted: 11 August, 2024; Published: 08 April, 2025

Abstract: This work comprehensively analyses the device physics of a charged plasma-doped $InGaAs_{5.86}GaAs_{5.65}$ Tunnel field effect transistor (TFET) biosensor featuring a dual metal gate configuration. The device is simulated using Silvaco Atlas TCAD, with HfO_2 employed as the gate dielectric alongside a nanocavity to enhance biosensing performance. The investigation focuses on crucial device parameters, including energy band profiles, potential distribution, electric field variations in both lateral and vertical directions, and electron concentration dynamics. Outcomes indicate that the biosensor keeps a superior response in the ambipolar region, with a drain current (I_D) or an on current (I_{ON}) of ~10^{-4}, due to the amalgam of the dual metal gate and InGaAs/GaAs heterostructure. This configuration also assists in supervising the flow of the carriers and, therefore, improves biosensing sensitivity and specificity. The results emphasize the advantage of this TFET configuration for next-generation biosensing technologies.

Index Terms: Ambipolar, Biosensor, Dual Metal Gate, Heterostructure, TFET, Tunnel Field Effect Transistor

1. Introduction

Innovation in semiconductor devices has been spurred by the quick development of biosensing technologies, especially in the detection of biomolecules with exceptional selectivity and sensitivity. Their unique structure helps facilitate steep sub-threshold slopes and curtailed power consumption, and tunnel field effect transistors (TFETs) have emerged as promising candidates [1]. This enhances their utility in sensitive biosensing applications. More specifically, it has been depicted that the use of heterostructures, such as *InGaAs/GaAs*, refines the transport of carriers and the band alignment, which in turn prepares the ground for enhanced TFET configuration [2]. Even more accurate control of the device is obtained without the need for ion implantation, particularly in combination with advanced ion doping techniques using charge plasma doping [3].

Recently, the use of dual metal gate topologies drew attention because it enabled unilateral alteration of the drain and source regions, which amended the electrostatic stability of the channel [4]. Combining this dual gate structure with an *InGaAs/GaAs* heterostructure charged plasma doped makes for a good strategy for improving the efficiency of the TFET-incorporated biosensor [5]. Further, the device performance can be further enhanced agnostically by incorporating a nanocavity in the lateral vicinity of the channel region along with high-k dielectrics such as HfO_2 in the gate stack. This discovery has relevance beyond the academic sphere to many fields, such as chemical detection, environmental protection, and health services [6]. Establishing sensitivity of the proposed TFET biosensor with the capability of detecting some forms of biomolecules can also be beneficial in healthcare, where disorders can be diagnosed timely and treated appropriately, customizing the therapy to the patient. This can also extend to supervising pollution control measures in which pollutants and toxins are scanned precisely, thus observing public health safety and

law requirements [7]. The improved performance of biosensors in chemical detection can also provide an opportunity to develop low-power portable monitoring instruments for hazardous substances with real-time capability, which is an important development for industrial safety and security issues.

1.1 Practical Applications of the Dual Metal Gate TFET Biosensor

For instance, by establishing two case studies where this TFET biosensor is used in factory settings to monitor the treatment of harmful chemicals, such as hydrogen sulfide and ammonia, due to their negative environmental impacts on human health in a contextual manner. Ordinary sensors usually face challenges such as low sensitivity and long lag periods. By virtue of the high-k dielectric layer and the nanocavity architecture, the proposed biosensor will be able to detect even minimal concentrations of these gases since it will detect a tiny change in their molecular presence. This ability would facilitate rapid response to exposure and detection, helping companies meet environmental requirements and protect employees and communities where the companies operate.

Next, we throw light on a medical scenario where the suggested InGaAs/GaAs TFET biosensor has the potential to be utilized in a therapeutic context for the early identification of cancer biomarkers that are present in blood serum at incredibly low quantities. These biomarkers are difficult to identify by conventional diagnostic techniques because of their significant background noise and low sensitivity. Nevertheless, this biosensor may attain an elevated ON-state current of 10^{-4} A/μm by utilizing the unique dual metal gate structure with charge plasma doping, guaranteeing improved sensitivity and selectivity [8,9,10,11,12,15,16]. Therefore, early cancer detection could facilitate timely diagnosis and therapy, enhancing patient outcomes and the likelihood of survival.

1.2 Research gaps

Key research gaps include: (1) investigating the potential of dual metal-gate heterostructures with charge plasma doping nanomaterials for ambipolar TFET biosensors; (2) establishing the sensitivity and high on-current of TFET biosensors for biomolecule detection; and (3) exploring the impact of nanocavity integration on the electrostatic potential and carrier distribution in these devices.

1.3 Problem statement

While advancements have been made in TFET biosensors, their performance remains limited by conventional doping methods, single metal gate configurations, and the under-exploration of heterostructure materials and nanocavity integration. This results in suboptimal on-current and sensitivity, particularly for ambipolar applications.

1.4 Main focus and objectives

Based on the identified research gaps, the primary objectives of the work are as follows:

i. To develop and optimize dual metal-gate heterostructure TFET biosensors incorporating charge plasma doping nanomaterials.
ii. To quantify the sensitivity and on-current of TFET biosensors for the detection of various biomolecules.
iii. To investigate the influence of nanocavity integration on the electrostatic potential, carrier distribution, and overall performance of TFET biosensors.

1.5 Manuscript organization and structure

The manuscript follows a structured organization comprising five main sections, each with a specific purpose in elucidating the Dual gate charge plasma doped InGaAs/GaAs Heterostructure TFET Biosensor. Section 1 introduces the readers to the importance and the impact of the particular heterostructure combination with dual gates and the use of the high-k dielectric (HfO_2). The impact of the research in the modern era has also been highlighted. Lastly, it concludes with the research gaps and the problem statement of the manuscript, which deals with how to rectify the same. Moving to Section 2, the device architecture and simulation part highlights the device specifications considered, the heterostructure's lattice matching calculation, structure, materials and the simulation environment taken with Silvaco Atlas TCAD. Section 3 reports experimental results, detailing calibration of the transfer characteristics of the device as well as studying the device physics characteristics. Section 4, the conclusion part, summarizes the key findings, underscoring the biosensor's behaviour over different parameters and superiority in the ambipolar zone. Lastly, section 5 concludes with potential avenues for future research and development, offering further exploration and enhancement directions. This meticulous arrangement guides readers through a coherent progression, facilitating a comprehensive understanding of the novel architecture's development, application, and future prospects.

2. Proposed Model and Device Specifications

This section outlines the key contributions of this manuscript, including the proposed model, methodology, mathematical framework, model specifications, and parameter specifications.

2.1 Methodology

The research methodology illustrated in the image of Fig.1 starts by outlining the device design specifications and then the simulation environment construction within Silvaco Atlas. Once the simulation framework is set up, the next step is describing the heterostructure mathematically, followed by detailed device physics. Following an analytical prejudice, if the results from the analysis are validated by successfully replicating some previously performed work, then the study may progress into performance comparison with particular emphasis on the study of ambipolar state. When such results are devoid of these validation criteria, the process shall be reconvened afresh from the design specification stage.

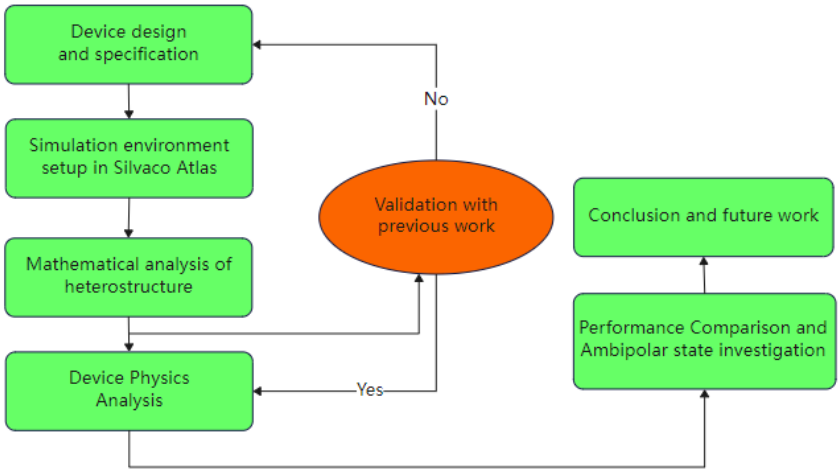

Fig. 1. Methodology of the proposed work.

The Charge Plasma-Doped InGaAs/GaAs Tunnel Field Effect Transistor (TFET) biosensors with a dual metal gate configuration were designed with specific device parameters as outlined in Table 1. The source length (L_S), cavity length (L_C), drain length (L_D), and gate length (L_G) are key structural components that define the physical dimensions of the device. The gate work function (ϕ_G) governs the gate's ability to control the channel, while the source and drain work functions (ϕ_S and ϕ_D, respectively) play crucial roles in modulating carrier transport. Additionally, doping concentrations are crucial in determining device performance, with the source doping concentration (N_S), drain doping concentration (N_D), and channel doping concentration (N_{CH}) precisely controlled to optimize the device's electrical characteristics. These parameters were carefully chosen to enhance the ambipolar response and sensitivity of the biosensor, facilitating its application in biomolecule detection.

Table 1. Device specifications

Serial No.	Parameters	Symbols
1	Source Length	L_S
2	Cavity Length	L_C
3	Drain Length	L_D
4	Gate Length	L_G
5	Gate Work Function	ϕ_G
6	Source and Drain Work Function	ϕ_S, ϕ_D
7	Source doping Concentration	N_S
8	Drain doping Conc.	N_D
9	Channel doping Conc.	N_{CH}

In Table 2, the variable and parameter definitions are provided, where specific values are assigned to each parameter for the Charge Plasma-Doped InGaAs/GaAs TFET biosensor with a dual metal gate configuration; these parameters are much impactful for achieving the desired electrical characteristics and sensitivity in biomolecule detection.

Table 2. Variable and Parameter Definition

Serial No.	Symbols	Values
1	L_S	10nm
2	L_C	5nm
3	L_D	10nm
4	L_G	20nm
5	ϕ_G	4.2eV
6	ϕ_S, ϕ_D	4.2eV
7	N_S	$1 * 10^{20}/cm^3$
8	N_D	$1 * 10^{18}/cm^3$
9	N_{CH}	$1 * 10^{19}/cm^3$

2.2 Mathematical model

To sum up, implementing the proposed TFET biosensor involved several mathematical challenges, particularly in optimizing the dual-metal gate alignment, accurately modelling the heterostructure, and calibrating charge plasma doping. The uniform electric field is shown in Equation 1,

$$E = V_{GS} / d \tag{1}$$

Careful adjustments to gate spacing were required to ensure consistent performance across the channel. For the InGaAs/GaAs heterostructure, the lattice constant was determined using Vegard's Law, minimizing strain, using equation 2,

$$\epsilon = \frac{a_{InGaAs} - a_{GaAs}}{a_{GaAs}} \tag{2}$$

to prevent defects. Furthermore, charge concentration *n* was calculated using equation 3, enabling precise control over doping levels.

$$n = N_D . \frac{1}{1 + \frac{N_D}{N_A}} \tag{3}$$

The On-current illustrated in equation 4, further demonstrated how adjustments in doping influenced conductivity while minimizing leakage currents. These mathematical insights were crucial for refining the biosensor's design and optimizing its performance.

$$I_{ON} = q.n.A.\mu.E \tag{4}$$

Another issue was achieving an optimal alignment and balance between the metal gates to ensure uniform electric field distribution. Any misalignment or imbalance could lead to non-uniform potential gradients, adversely affecting the device's performance. This was mitigated by conducting extensive simulations to fine-tune the placement and dimensions of the gates, ensuring a stable and well-distributed electric field across the channel.

Fig.2 illustrates the intricate architecture of the suggested device, dual gated charge plasma Doped $InGaAs_{(1-x)}GaAs_x$ Tunnel FET Biosensors integrated with nanocavity, engineered specifically regarding biosensing applications. This device showcases a well-defined composition, comprising five distinct main regions that contribute to its functionality along with high- k dielectric hafnium dioxide (HfO_2); these regions encompass the source, drain, and channel, designated by their vivid yellow hue for GaAs, along with the Oxide region, distinctly highlighted in blue. The InGaAs region is depicted in orange for the source. The device also comprises a pair of dual metal gate electrodes and, notably, an individual source and drain electrode, each surrounded by a delicate, slender green line line, as meticulously depicting the SiO2 (Silicon dioxide) to avoid silicide formation.

The dual metal gate arrangement significantly improves the biosensor's productivity, which combines charge plasma doping with a nanocavity on one side and HfO_2 on the other. Because any variations in the dielectric environment surrounding the cavity influence the channel's electric field and carrier concentration, the nanocavity improves sensitivity by enabling accurate biomolecule recognition. The opposite gate's high-k HfO_2 dielectric promotes gate capacitance, lowers leakage, and strengthens the gate-to-channel coupling to optimize gate control. When combined with charge plasma doping, this dual gate technique allows for the independent manipulation of the source and drain regions, improving the device's ambipolar nature and increasing the ON-state current. As a result, this design is extremely efficient in detecting biomolecules at modest concentrations in a variety of scenarios due to its improved electrostatic control, lower power intake, and increased biosensing sensitivity.

An InGaAs/GaAs heterostructure is a distinctive feature of this innovative design, combining indium gallium arsenide (InGaAs) and gallium arsenide (GaAs) to leverage their complementary properties. This heterostructure enables the formation of energy bands that promote efficient electron tunnelling, which is crucial for improving the transistor's speed and energy efficiency. The deliberate selection of these materials reflects an intentional effort to advance conventional semiconductor device design. Additionally, the introduction of charge plasma doping adds another layer of complexity.

The device's electrical properties can be precisely controlled by carefully incorporating charged particles into the semiconductor. This process enhances the transistor's conductivity and regulates the flow of charge carriers, ultimately leading to superior overall performance. The implementation of charge plasma doping highlights a sophisticated strategy to fine-tune the transistor's characteristics for optimal functionality.

The unique attributes of this innovative structure—including the integration of a nanocavity paired with a dual metal gate and high-k dielectric (HfO_2), the InGaAs/GaAs heterostructure, and charge plasma doping, represent a significant evolution in TFET design. This shift from traditional approaches underscores a commitment to enhancing tunnel field-effect transistors' performance, emphasizing precision, efficiency, and refined control of electronic processes at the nanoscale. The source and drain regions are meticulously designed with dimensions of 10 nm each, optimized for their specific roles. The nanocavity, a crucial element for biosensing, is precisely configured at 5 nm in length to effectively capture target molecules. The channel, which plays a key role in determining the device's conductive properties, extends over 20 nm, integrating these elements into a cohesive and well-balanced architecture.

Table 1 provides the specifications for the proposed device architecture of dual gated charge plasma doped $InGaAs_{(1-x)}GaAs_x$ Heterostructure TFET Biosensor with the prevalent devices. For the heterostructure, the combination of $InGaAs_{(1-x)}GaAs_x$ has been chosen in order to control the strain issues with a lattice constant of 5.86 Å, calculated from Vegard's Law [13], portrayed in equation 6,

$$a_{InGaAs_{(1-x)}GaAs_x} = x_{a_{InAs}} + (1-\mathrm{x})a_{GaAs} \tag{5}$$

Where x represents the mole fraction of InAs in the alloy, ranging from 0 to 1, InGaAs, with a superior electron affinity (4.2 eV) compared to GaAs (4.07 eV), form a type I heterostructure with staggered band alignment. In this configuration, the conduction band minimum of InGaAs is lower than that of GaAs, creating an electron potential well in the former region. This configuration confines electrons within the first layer, resulting in a type I heterostructure with compressive strain due to the lattice mismatch. Such compressive strain can induce the formation of a quantum well structure characterized by quantized energy levels. The strain-induced bandgap modifications significantly enhance carrier confinement within the quantum well, thereby improving the mobility of InGaAs. A comprehensive set of parameters has been carefully selected and listed in Table 1 for precise simulation and analysis. These specifications provide a detailed framework for understanding the operational dynamics of the proposed device, playing a crucial role in evaluating and validating its performance during simulations.

Fig.2 and its corresponding descriptive annotations outline a pioneering device configuration that fuses the principles of a Tunnel Field Effect Transistor (TFET) with the innovation of a Nano cavity and high-k dielectric, supported with dual gate, all geared towards facilitating advanced biosensing employments. This amalgamation of meticulously designed components and carefully selected dimensions promises to deliver heightened sensitivity and specificity, potentially revolutionizing the field of molecular detection and analysis [14].

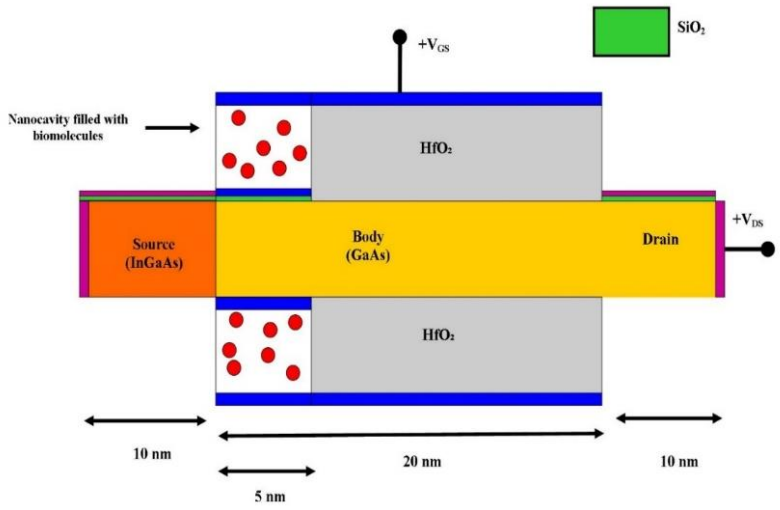

Fig. 2. 2-D structure of dual gated charge plasma doped $InGaAs_{5.86}GaAs_{5.65}$ Tunnel FET Biosensor.

2.3 Limitations of the mathematical model

The mathematical model for the proposed TFET biosensor faces certain limitations, primarily due to the complexity of accurately capturing real-world conditions through equations. For instance, Vegard's Law simplifies the lattice constant calculation, but in practice, factors like non-uniform strain distribution and defects can deviate from ideal assumptions, affecting performance predictions. Additionally, the uniform electric field assumption in equation (1) overlooks potential local variations in electric fields due to imperfections in gate alignment or material interfaces, which could lead to inconsistent device behaviour. Moreover, while charge plasma doping is mathematically modelled to control carrier concentration, variations in doping efficiency or unintended doping gradients could affect the accuracy of current calculations, as reflected in equation (4). These limitations highlight the challenge of ensuring model precision when simulating complex heterostructure-based devices with nanoscale features.

Few assumptions can be made to eradicate these voids, such as advanced simulation techniques, like atomistic modelling or multi-physics simulations, can be employed to capture real-world imperfections. Additionally, experimental calibration of the model with real device data will help fine-tune assumptions and improve accuracy.

3. Simulation and Results Analysis

This section presents the simulation environment for the Charge Plasma-Doped InGaAs/GaAs TFET biosensor, which was developed using Silvaco Atlas TCAD. The transfer characteristics are calibrated to ensure accurate modelling of the device's electrical behaviour. The results are compared with those of a conventional nanotube TFET, highlighting key differences in performance. Special attention is given to the ambipolar region, where the dual metal gate configuration demonstrates reduced ambipolar currents. The calibrated simulations provide deeper insights into the enhanced sensitivity and overall performance of the biosensor for biomolecule detection.

3.1 Simulation

In the Charge Plasma-Doped InGaAs/GaAs TFET biosensor simulation, several advanced models were used in Silvaco Atlas TCAD to reflect the device's behaviour accurately. The "btbt. Nonlocal" model (a model of SILVACO Atlas TCAD) was employed to capture the critical band-to-band tunnelling (BTBT) effects, which are central to TFET operation. This model considers spatial variations in the process for improved accuracy. The band gap narrowing (BGN) model was also included to account for the bandgap reduction in highly doped regions, impacting carrier injection and switching characteristics. Other essential models used include Shockley-Read-Hall (SRH) recombination to simulate carrier recombination via defect states and electric field-dependent mobility to account for the impact of electric fields on carrier transport. These models accurately represent the device's current-voltage characteristics, while the PRINT function provides detailed output for performance monitoring. Together, these models enable precise simulation of the TFET biosensor's device physics and biomolecule detection capabilities.

3.2 Results and discussions

This section deals with the device physics analysis of the proposed charge plasma doped dual metal gated InGaAs/GaAs TFET biosensor over the conventional nanotube TFET and the device's response in the ambipolar state. Fig. 3 shows the calibration curve comparing the proposed device's drain current (ID) or ON current (ION) with a conventional nanotube TFET. The proposed device achieves a significantly higher ON current of 10^{-4} A, while the traditional TFET exhibits a much-diminished value. Certain design aspects have mainly brought about this noteworthy advancement. The introduction of dual-metal gates assists in forming an asymmetric potential across the device and, therefore, aids in varying the tunnelling barrier. Adding a nanocavity next to the source region further enhances the electric field in the source-channel interface. This contributes to more excellent band bending and a smaller tunnelling barrier. Hence, there is more carrier tunnelling from the source to the channel. The InGaAs/GaAs heterostructure provides the benefit of better electron band alignment with lower effective mass and easy tunnelling. Increasing the carrier transport ability by charge plasma doping in the source and drain areas adds an enhanced conductive flow in ON current (drain current), thus improving the same. Collectively, these effects allow the device to deliver significantly better performance than conventional TFETs.

Fig. 4 displays the energy band diagram for the proposed and conventional nanotube TFETs. The proposed device shows a significantly steeper and narrower tunnelling barrier than the conventional TFET. This can be attributed to the optimized heterostructure of $InGaAs_{(1-x)}GaAs_x$, which offers a staggered band alignment. In this alignment, the conduction band minimum of InGaAs is lower than that of GaAs, creating a potential well that confines electrons in the InGaAs region. This confinement enhances electron density in the channel, improving tunnelling efficiency. The dual-metal gate design further modulates the channel's potential, reducing the tunnelling barrier's width and increasing the field across the junction. This configuration promotes a higher tunnelling rate, even at lower gate voltages. As a result, the proposed device shows better ON current (drain current) characteristics and more responsive and controllable switching behaviour, particularly in the ambipolar state where both electron and hole tunnelling processes are active. This enhanced control over carrier transport and tunnelling mechanisms is a key factor in the superior performance of the proposed TFET biosensor.

Fig. 5 presents the proposed device's vertical electric field distribution and the conventional nanotube TFET. The proposed device exhibits a significantly higher vertical electric field across the channel, even in the ambipolar state, whereas the conventional Tunnel FET shows an almost negligible vertical field. This enhancement in the vertical field is due to the unique dual-metal gate configuration and the integration of a nanocavity. The dual metal gates form an asymmetric electric potential across the vertical axes, which produces a solid vertical electric field when coupled to charge plasma doping. This field assists in effectively modulating the potential barrier and thus increases the probability of tunnelling and carrier injection. Using the higher vertical electric field in the proposed device helps increase the efficiency and decrease the threshold voltage, enhancing the ability to switch the device.

Fig. 6 illustrates the proposed device's lateral electric field profile compared with the conventional nanotube TFET. The proposed device shows a much stronger lateral electric field response, almost zero compared to the conventional device. The enhanced lateral field in the proposed device is attributed to the optimized InGaAs/GaAs heterostructure and the strategic placement of the dual-metal gate, which results in a sharper potential gradient along the lateral direction. This configuration leads to better confinement and transport of charge carriers, reducing scattering and improving mobility. The increased lateral field also ensures better control over the channel, which is particularly beneficial in the ambipolar state, enhancing the device's sensitivity and reducing off-state leakage currents. This optimized electric field profile in both the vertical and lateral directions enables the proposed device to achieve superior performance metrics, including a higher ON current (drain current) and improved I_{on}/I_{off} ratio.

Fig. 7 depicts the proposed device's electron concentration profile compared to the conventional nanotube TFET. The behaviour of the suggested architecture is observed to be much better regarding the electron concentration in the channel and mainly in the ambipolar state, where its response is even more pronounced. This boost in electron concentration is attributed to the excellent design of the InGaAs/GaAs heterostructure that confines electrons within the quantum well in the channel region. The dual-metal gate configuration further enhances this effect by adjusting the electric field and, thus, carrier distribution more accurately. Additionally, charge plasma doping at the source and drain regions generates a higher carrier density, leading to improved conductivity and curtailed resistance in the channel. The enhanced electron concentration in the ambipolar state allows for more efficient tunnelling of carriers, resulting in improved ON current (drain current) and overall device performance compared to the conventional nanotube TFET. This increased carrier density is crucial for achieving high sensitivity and faster response times in biosensing applications. Table 2. shows the superiority of the suggested device architecture over the existing counterparts in the recent semiconductor domain.

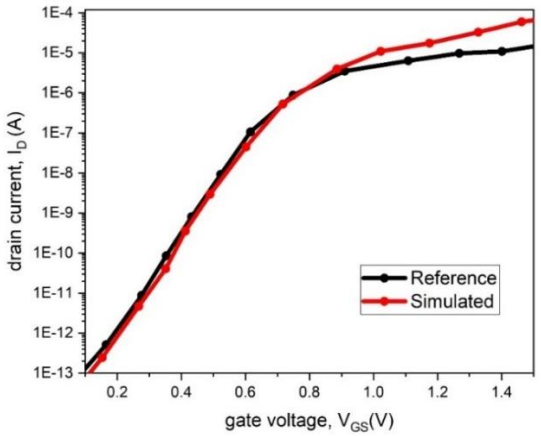

Fig. 3. Calibration curve: I_D vs. V_{GS} for proposed vs. conventional TFET.

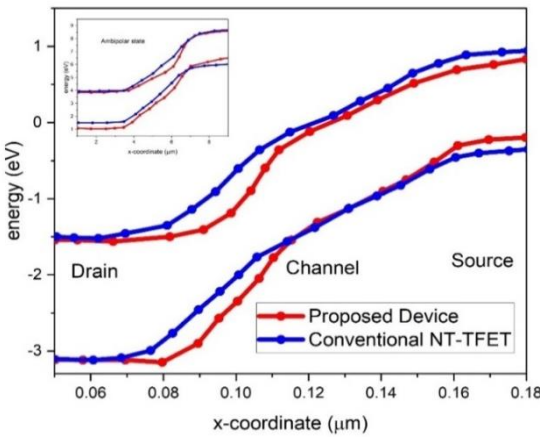

Fig. 4. Energy band variation: proposed vs. conventional TFET.

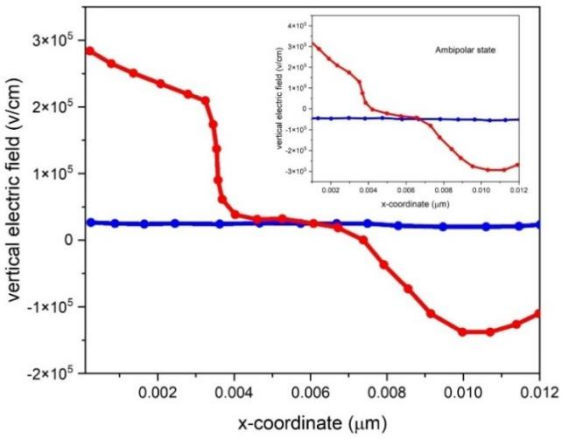

Fig. 5. Vertical electric field: proposed vs. regular TFET.

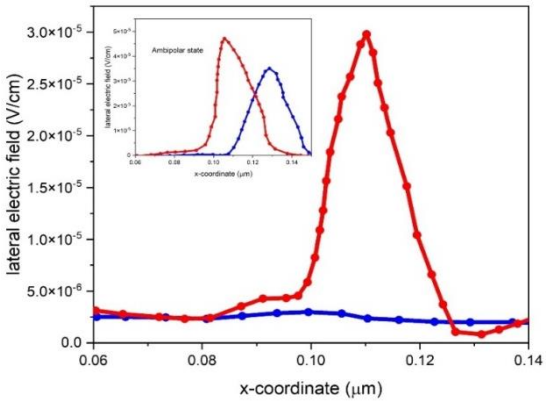

Fig. 6. Lateral electric field fluctuation: suggested vs. conventional device.

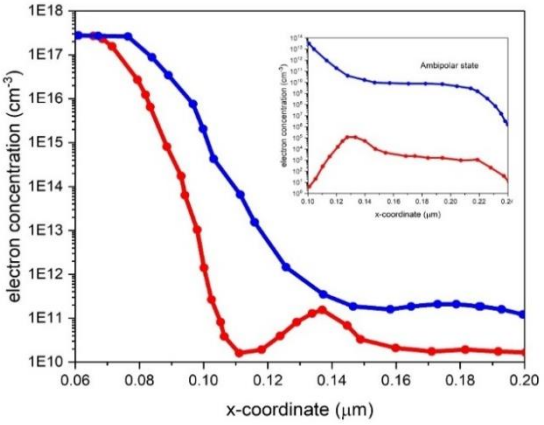

Fig. 7. Electron concentration: proposed vs. conventional TFET.

Table 3 presents existing devices' I_{ON} (on current), i.e., drain current (I_D) values alongside the proposed Charge Plasma-Doped InGaAs/GaAs TFET biosensor. The suggested device demonstrates a significantly improved current, reaching approximately 10^{-4} A, notably higher than the prevailing devices. This enhancement in I_{ON} is attributed to the optimized dual metal gate configuration and the advanced device design, which lead to more efficient carrier transport and reduced ambipolar effects, thereby improving the overall device performance in biosensing applications.

Table 3. Comparative table showcasing the I_{ON} of the prevailing devices alongside the proposed counterpart.

Works	I_{ON} (A/μm)
[4]	~10^{-8}
[5]	~10^{-6}
[6]	~ (10^{-7} to 10^{-6})
[7]	~10^{-6}
[8]	~10^{-8}
Suggested Work	~10^{-4}

3.3 Simulation challenges and rectification

In simulating TFET biosensors, many difficulties may emerge due to the complicated process of nanoscale device modelling. For instance, there is the problem of accurately defining the heterostructure with regard to lattice mismatches and strain that fosters defects, making modelling all the more difficult. Besides, modifying charging parameters in the TFET for optimal performance entails charge plasma doping, with each doping profile being optimally designed. Still, there is the problem of dual-metal gates being aligned, where misalignment produces undesirable electric field variations that may weaken the entire device. This process has several factors, but more attention is needed to optimize the device performance further using advanced computational methods that mesh and converge optimally with the architecture and material properties of the device.

A number of strategies were adapted to meet the simulation issues. When it came to modelling the heterostructure, advanced material simulation techniques like multi-scale modelling were incorporated to minimize defects caused by lattice mismatch and strain. The charge plasma doping process was advanced by implementing accuracy on doping profiles and tuning the parameters with experiments using a charge carrier concentration control. In order to avoid improper alignment of the dual-metal gate, several simulations were carried out with the gates of different sizes and placements to achieve the optimum uniformity of the electric field along the channel. Similarly, compressing time and solving accuracy problems were accomplished by using adaptive meshing techniques and parallel computing devices for faster convergence and reduced simulation time.

4. Conclusion and Future Scope

To conclude, the suggested $InGaAs_{5.86}GaAs_{5.65}$ Tunnel FET biosensor with charge plasma doping and a dual metal gate architecture exhibits markedly enhanced efficiency parameters, such as a high ON current (drain current) of 10^{-4} A/μm and a remarkable I_{on}/I_{off} ratio of ~10^{1} A/μm. The novel device architecture, which maximizes the electron concentration and electric field distribution in the channel region, is primarily responsible for these improvements. In addition to increasing carrier mobility, the deliberate addition of a high-k dielectric (HfO_2) and nanocavity to the heterostructure helps create a more consistent electric field, facilitating effective electron tunnelling. Vegard's law might not adequately account for strain effects and lattice aberrations in the InGaAs/GaAs heterostructure since it presupposes a linear relationship between lattice constants and composition. Furthermore, this model ignores alloy content fluctuations and bending implications, both of which can affect electrical traits.

Furthermore, strain-induced modifications to band alignment and energy gaps are not taken into consideration. These restrictions point to the necessity for improved modelling and validation through experiments. Improved ambipolar behaviour is a consequence of this configuration's efficient suppression of leakage currents and reduction of off-state power consumption. These design features work in concert to create a sturdy and responsive biosensor, showcasing its potential for high-sensitivity biomolecular detection and cutting-edge electronic usage.

Although the suggested dual metal gated charge plasma InGaAs/GaAs TFET biosensor has great promise for biomolecular detection, several aspects still need further investigation and improvement. Experiments with different nanocavity dimensions and various high-k dielectrics may be conducted to improve sensitivity and specificity for a larger class of biomolecules. Two-dimensional materials like graphene or MoS_2 could be incorporated into the heterostructure to enhance device performance and carrier mobility. To improve its applicability for point-of-care diagnostics, future research should concentrate on integrating the biosensor with microfluidic devices for real-time, on-chip detection. To close the gap between theory and real-world applications, real biomolecules must be fabricated and tested as part of an experimental validation process for the simulation results. Furthermore, these sensors will need to be developed into effective, low-power readout circuits and interfaces to be used in portable diagnostic tools and Internet of Things-based health monitoring systems.

References

[1] Jeyanthi, J.E., Samuel, T.S.A., Geege, A.S, Vimala, P. (2022). A detailed roadmap from single gate to heterojunction TFET for next generation devices. *Silicon*, vol. 14, pp. 3185-3197. doi: 10.1007/s12633-021-01148-7.

[2] Ghosh, S., Venkateswaran, P., Sarkar, S.K. (2024), Analysis of circuit performance of Ge-Si hetero structure TFET based on analytical model. *Circuit World*, vol. 50, no. 2/3, pp. 195-204. doi: 10.1108/CW-08-2020-0175.

[3] Keighobadi, D., Mohammadi, S., Mohtaram, M. (2022). Recessed gate cylindrical heterostructure TFET, a device with extremely steep subthreshold swing. *Transactions on Electrical and Electronic Materials*. vol 23, pp. 81-87. doi: 10.1007/s42341-021-00321-4.

[4] Basab, D., Bhowmick, B. (2023). Dielectrically modulated ferroelectric-TFET (Ferro-TFET) based biosensors. *Materials Science and Engineering: B*, vol. 298, pp. 116841. doi: 10.1016/j.mseb.2023.116841.

[5] Rajesh, S., Hirpara, Y., Hoque, S. (2021). Sensitivity analysis on dielectric modulated Ge-source DMDG TFET based label-free biosensor. *IEEE Transactions on Nanotechnology*. vol. 20, pp. 552-560. doi: 10.1109/TNANO.2021.3093927.

[6] Peesa, R.B., Panda, D.K. (2022). Rapid detection of biomolecules in a junction less tunnel field-effect transistor (JL-TFET) biosensor. *Silicon*. vol. 14, no. 4, pp. 1705-1711. doi: 10.1007/s12633-021-00981-0.

[7] Agnihotri, S.K., Samajdar, D.P., Rajan, C., Yadav, A.S., Gnanesh, G. (2020). Performance analysis of gate engineered dielectrically modulated TFET biosensors. *International Journal of Electronics*. vol. 108, no. 4, pp. 607-622. doi: 10.1080/00207217.2020.1793407.
[8] Wang, Y., Li, C., Li, O., Cheng, S., Liu, W., You, H. (2022). Simulation study of dual metal-gate inverted T-shaped TFET for label-free biosensing. *IEEE Sensors Journal*. vol.22, no. 19, pp. 18266-18272. doi: 10.1109/JSEN.2022.3195180.
[9] Hur, J., Moon, D.-I., Han, J.-W., Kim, G.-H., Jeon, C.-H., Choi, Y.-K. (2017). Tunneling effects in a charge-plasma dopingless transistor. *IEEE Transactions on Nanotechnology*. vol. 16, no. 2, pp. 315-320, doi: 10.1109/TNANO.2017.2663659.
[10] Kumar, R., Kumar, J., Devi, L.V., Singh, K. (2023). Comparative study of doped and doping less charge-plasma silicon microstrip detector, Materials Today: Proceedings, vol. 80, part 3, pp. 1801-1805. doi: 10.1016/j.matpr.2021.05.614.
[11] Mishra, V., Verma, Y.K., Gupta, S.K., Rathi, V. (2022). A SiGe-source doping-less double-gate tunnel FET: design and analysis based on charge plasma technique with enhanced performance. *Silicon*. vol. 14, pp. 2275–2282. doi: 10.1007/s12633-021-01030-6.
[12] Singh, S., Chauhan, A.K.S., Joshi, G. Singh, J. (2022). Design and investigation of SiGe heterojunction based charge plasma vertical TFET for biosensing application. *Silicon*, vol. 14, pp. 6193–6204. doi: 10.1007/s12633-021-01384-x.
[13] Denton, A. R., Ashcroft, N. W. (1991). Vegard's law. *Physical review A*, vol. *43*, no. 6, pp. 3161. doi: 10.1103/PhysRevA.43.3161.
[14] Manual, A. U. (2000). Silvaco International. *Santa Clara, CA*, *95054*, 23.
[15] Vimala, P., Krishna, L.L., Sharma, S.S. (2022). TFET biosensor simulation and analysis for various biomolecules. *Silicon*, vol. 14, pp. 7933–7938. doi: 10.1007/s12633-021-01570-x.
[16] Sakthivel, R., Keerthi, M., Chung, R.-J., He, J.-H. (2023). Heterostructures of 2D materials and their applications in biosensing. *Progress in Materials Science*, vol. 132, pp. 101024. doi: 10.1016/j.pmatsci.2022.101024.

Authors' Profiles

Soumya Sen received his Master's degree in Microelectronics and VLSI Technology from West Bengal University of Technology, Kolkata, West Bengal, India and pursuing his PhD from Dr. B. R Ambedkar National Institute of Technology Jalandhar, Punjab with specialization in Nanoelectronics. He is currently an Assistant Professor in the Department of Computer Science & Engineering at the University of Engineering & Management, Jaipur, India. His research interests include and VLSI design, Nanostructures (Tunnel FETs, Nanotubes, Nanowires) and modelling of devices.

Angshuman Khan is currently an Associate Professor in the Department of Electronics & Communication Engineering at the University of Engineering & Management, Jaipur, India. He earned his Ph.D. from the National Institute of Technology Patna (NIT Patna), Bihar. His primary research interests include nanocomputing, VLSI circuit design, WSN, artificial neural network, device modelling, and simulation.

How to cite this paper: Soumya Sen, Angshuman Khan, "Optimized Ambipolar Characteristics in Charge Plasma-Doped InGaAs/GaAs TFET Biosensors with Dual Metal Gate", International Journal of Engineering and Manufacturing (IJEM), Vol.15, No.2, pp. 36-45, 2025. DOI:10.5815/ijem.2025.02.03